Spectroscopic investigation of H atom transfer in a gas-phase dissociation reaction: McLafferty rearrangement of model gas-phase peptide ions†

Michael J. Van Stipdonk,*[a] Dale R. Kerstetter,[a] Christopher M. Leavitt,[a] Gary S. Groenewold,[b] Jeffrey Steill[c] and Jos Oomens[c]

Received 11th February 2008, Accepted 27th March 2008
First published as an Advance Article on the web 23rd April 2008
DOI: 10.1039/b802314j

Wavelength-selective infrared multiple-photon photodissociation (WS-IRMPD) was used to study isotopically-labeled ions generated by McLafferty rearrangement of nicotinyl-glycine-*tert*-butyl ester and betaine-glycine-*tert*-butyl ester. The *tert*-butyl esters were incubated in a mixture of D_2O and CH_3OD to induce solution-phase hydrogen-deuterium exchange and then converted to gas-phase ions using electrospray ionization. McLafferty rearrangement was used to generate the free-acid forms of the respective model peptides through transfer of an H atom and elimination of butene. The specific aim was to use vibrational spectra generated by WS-IRMPD to determine whether the H atom remains at the acid group, or migrates to one or more of the other exchangeable sites. Comparison of the IRMPD results in the region from 1200–1900 cm^{-1} to theoretical spectra for different isotopically-labeled isomers clearly shows that the H atom is situated at the C-terminal acid group and migration to amide positions is negligible on the time scale of the experiment. The results of this study suggest that use of the McLafferty rearrangement for peptide esters could be an effective approach for generation of H-atom isotope tracers, *in situ*, for subsequent investigation of intramolecular proton migration during peptide fragmentation studies.

Introduction

Fragmentation of gas-phase, protonated peptide ions during collision-induced dissociation (CID) under low-energy conditions (*i.e.* 1 to tens of eV collision energy) involves extensive intramolecular rearrangement reactions that include cyclization, nucleophilic attack and proton transfer/migration.[1–10] In the gas-phase, peptides that contain basic amino acids such as histidine, lysine or arginine are assumed to be initially protonated at the respective side groups. For peptides that lack these basic residues, theoretical and experimental evidence exists for a mix of protonation sites that includes the amino-terminus and amide carbonyl oxygen atoms.[11,12] In most low-energy peptide dissociation reactions, amide bond cleavage requires the migration of the added proton, from the most basic site, to the point of nucleophilic attack and this general idea makes up the "mobile-proton" model of peptide dissociation.[13–25]

The general features of the mobile-proton model have been augmented recently to generate the "pathways in competition" model,[26] which takes into consideration a more comprehensive set of pre-dissociation and post-dissociation processes as well as the energies of reactive configurations, intermediates and transition states. In the mobile-proton and pathways in competition models, formation of a 5-, and in some cases 6-member cyclic intermediate is thought to be an integral part of the dissociation reactions.[2,3,6–10] For example, we recently incorporated alternative amino acids such as β-alanine (βA), γ-aminobutyric acid (γABu), ε-aminocaproic acid (Cap), and 4-aminomethylbenzoic acid (4AMBz) into model peptides, to determine the effect on fragmentation patterns of changing the size of the putative cyclic intermediate formed during the nucleophilic attack.[27] For protonated peptides, the presence of βA, γABu or Cap into the sequence XAAG, AXAG, and AAXG (where X represents the position of the "alternative" amino acid) inhibited or completely suppressed formation of specific b_n^+ and y_n^+ ions.[27] This observation was attributed to the prohibitive effect of forcing intramolecular nucleophilic attack and concomitant cyclization to proceed through larger cyclic intermediates, which should be kinetically slower to form and entropically less favored, when amino acids such as βA, γAbu or Cap were used. Cyclization is prohibited when the residue is 4AMBz because the rigid aromatic ring separates the nucleophile from the electrophilic site of attack.

[a] *Wichita State University, Wichita, KS, USA. E-mail: mike.vanstipdonk@wichita.edu; Fax: +1 316 978 3431; Tel: +1 316 978 7381*
[b] *Idaho National Laboratory, Idaho Falls, ID, USA. E-mail: gary.groenewold@inl.gov; Fax: +1 208 526 8541; Tel: +1 208 526 2803*
[c] *FOM Instituut voor Plasmafysica, Nieuwegein, The Netherlands. Fax: +31 30 6031 204; Tel: +31 30 6096 999*

† Electronic supplementary information (ESI) available: Tandem mass spectra for the dissociation of $(BetGOtBu)^+$ and $(BetGOH)^+$ (Fig. S1); tandem mass spectra generated from fully deuterium-exchanged betaine-glycine-*tert*-butyl ester using the quadrupole ion trap mass spectrometer (Fig. S2); comparison between IRMPD spectrum generated from $(NicGGOH^+H)^+$ and theoretical spectra based on DFT calculations for the structures studied (Fig. S3). See DOI: 10.1039/b802314j

Understanding clearly the relative importance of cyclization, nucleophilic attack and proton transfer to the yield of sequence ions during peptide fragmentation is important, as current protein identification in proteomics relies heavily on CID and tandem mass spectrometry to characterize peptides derived from enzymatic digestion. In many MS/MS experiments, fragment ion spectra are interpreted using bioinformatics tools in which sequencing algorithms and peptide fragmentation models are converged.[26] One problem, however, is that existing sequencing programs are based on rather limited fragmentation models that may not take into consideration the diverse and complex dissociation reactions of gas-phase peptide ions.[28] Clearly, a better understanding of the mechanisms behind peptide fragmentation during CID will improve the ability to use bioinformatics approaches for rapid and accurate identification.

In a prior study we demonstrated that CID of metal cationized peptides containing C-terminal *tert*-butyl ester groups causes McLafferty-type rearrangement[29] to generate products ions with a C-terminal acid group (Scheme 1). The rearrangement is depicted in Scheme 1 as a concerted process. For analogous Norrish type II reactions of neutral molecules,[30] and McLafferty-rearrangement of odd-electron ions,[31] there is compelling evidence of a two-step process that involves formation of a distonic radical. It is not clear whether the McLafferty-rearrangement of the peptide esters is concerted or stepwise, and mechanistic details of the process are not provided by conventional mass spectrometric experiments. The salient point, however, is that the reaction leads to the transfer of a γ-position H atom and elimination of an alkene.

Subsequent to our initial study, it was discovered that the McLafferty-type rearrangement can be used to generate an H isotope label in the gas-phase.[32] This isotope label could then serve as a tracer to determine the extent to which scrambling of protons about exchangeable sites along a peptide backbone may occur during CID. The ability to monitor the intramolecular migration and scrambling is desirable given the importance of migration of specific protons during peptide dissociation reactions noted above. In addition, scrambling of H and D during CID of peptides and proteins, which is well documented,[33–41] may degrade the accuracy of tandem hydrogen/deuterium exchange (HDX)/CID experiments to probe gas-phase conformation of peptides and proteins by mass spectrometry.[33,34,41]

In the method developed in the previous work, the isotope label is presumably generated at the C-terminal acid group by McLafferty rearrangement. Migration of the isotope label to other exchangeable sites after McLafferty rearrangement (intramolecular H/D scrambling), but prior to activation of a subsequent fragmentation reaction would negate the advantage of generating the label at a specific position. While there was clear evidence in the earlier study that scrambling of exchangeable H atoms *does* occur during dissociation reactions to produce sequence ions, what was not clear was the extent to which the isotope label may have migrated subsequent to the McLafferty rearrangement.

Ideally, the propensity for H atom migration could be determined using vibrational spectroscopy of isotopically-altered species, because molecular vibrations are very sensitive to changes in the reduced mass of the chromophores.

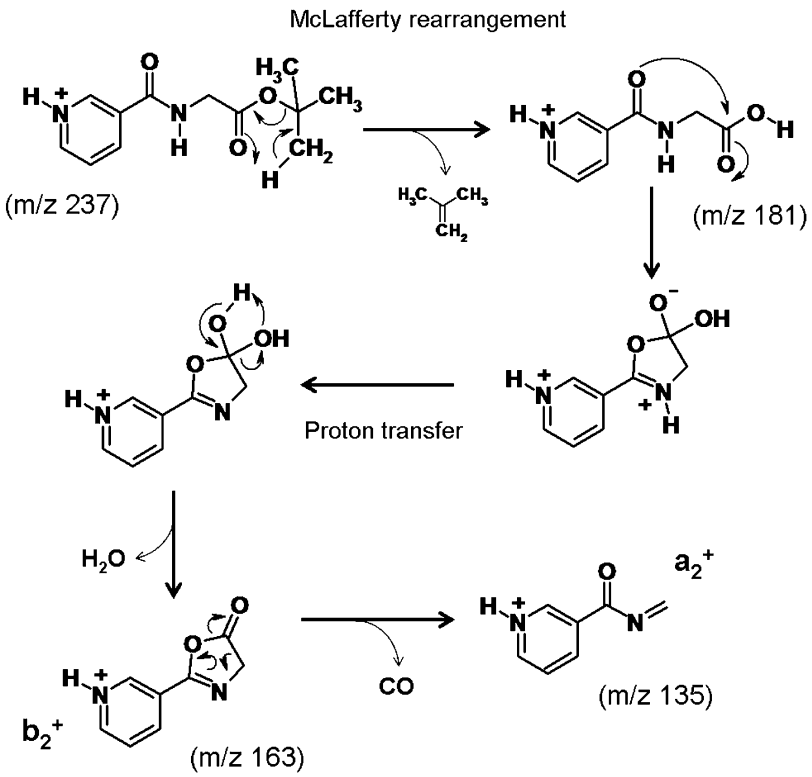

Scheme 1 Dissociation pathway for $(NicGO^tBu+H)^+$ showing McLafferty rearrangement and formation of b_2^+ and a_2^+ *via* the "oxazolone" pathway.

Photodissociation using IR free-electron lasers (FEL) has provided unprecedented access to the vibrational spectra of discrete, neutral or ionic gas-phase biomolecules through a large portion of the mid-infrared spectrum, including the diagnostic amide I and amide II regions.[9,10,12,42–52] Acquisition of conventional linear absorption spectra from peptide and protein ions typically studied using mass spectrometry is not practicable because of the extremely low ion densities (*i.e.* low absorber concentrations). However, using an action spectroscopy approach that combines an FEL and ion-trapping mass spectrometry, photon absorption can be monitored by measuring fragmentation yields from WS-IRMPD.[53–56]

We present here a study of the product ions generated following McLafferty-rearrangement of two model peptide systems: nicotinyl-glycine-*tert*-butyl ester (NicGO*t*Bu) and betaine-glycine-*tert*-butyl ester (BetGO*t*Bu$^+$). The peptide *tert*-butyl esters were incubated in a mixture of D_2O and CH_3OD to induce solution-phase hydrogen-deuterium exchange and then converted to gas-phase ions using electrospray ionization (ESI). McLafferty rearrangement was used to generate the free-acid forms of the respective model peptides through transfer of an H atom and elimination of butene. The resulting peptide ions were then subjected to WS-IRMPD to produce a vibrational spectrum from 1200–1900 cm^{-1}. The specific aim was to use the photodissociation technique to determine whether the H atom remains at the acid group, or migrates to one of the exchangeable sites, thus probing directly the tendency for H/D scrambling. The experiments provide proof-of-principle results that demonstrate that the IRMPD approach can be used to study intramolecular H atom transfer, and establish that the McLafferty rearrangement of the peptide esters can be used to selectively label the C-terminus of a peptide for "isotope tracer" studies of intramolecular proton migration. While details of Norrish type II reactions have been revealed by elegant femtosecond spectroscopy studies,[30] and inferences made to the analogous McLafferty rearrangement, to the best of our knowledge this type of gas-phase reaction has not been studied using WS-IRMPD.

Experimental

Peptide synthesis

Nicotinic acid, betaine hydrochloride, glycine *tert*-butyl ester hydrochloride and glycine methyl-ester hydrochloride were purchased from Sigma-Aldrich (St. Louis, MO) and used as received. The nicotinic acid and betaine were coupled to glycine *tert*-butyl ester to make NicGO*t*Bu and BetGO*t*Bu$^+$ using a resin-bound carbodiimide (PS-Carbodiimide, Argonaut, Foster City CA) suspended in dichloromethane. After a minimum of 8 h, the resin was removed by filtration, the remaining solution evaporated to dryness and the resulting peptide esters used without further purification. The same synthetic approach was used to generate nicotinyl-glycine-methyl ester by coupling nicotinic acid to glycine methyl ester. The composition and sequence of the peptide esters was confirmed using ESI and multiple-stage CID of $^{109}Ag^+$ adducts, which is an effective approach for sequencing of peptides from the C-terminus in the gas phase.[57]

Quadrupole ion trap mass spectrometry

Quadrupole ion trap CID was investigated using a Finnigan LCQ^{Deca} ion trap mass spectrometer (Thermo Fisher Scientific, San Jose CA). Solutions of each peptide ester were prepared by dissolving the appropriate amount of solid material in a 1 : 1 (V : V) mixture of CH_3OH and H_2O or CH_3OD and D_2O to produce final concentrations of 10^{-3} M. A small abount of trifluoroacetic acid was added to enhance protonation of NicGO*t*Bu. The peptide-ester solutions were infused into the ESI instrument using the incorporated syringe pump at a flow rate of 5 μL min^{-1}. The atmospheric pressure ionization stack settings for the LCQ (lens voltages, quadrupole and octapole voltage offsets, *etc.*) were optimized for highest $(M)^+$, $(M+H)^+$ or $(M+D)^+$ ion intensity using the auto-tune routine within the LCQ Tune program. The spray needle voltage was maintained at +5 kV, N_2 sheath gas flow rate at approximately 0.375 L min^{-1} and the capillary (desolvation) temperature at 200 °C.

For CID studies, the precursor isolation widths used were 0.8–1.0 mass to charge (m/z) units to ensure the isolation and dissociation of single isotopic peak. The normalized collision energies (which define the amplitude of R.F. voltage applied to the end cap electrodes to induced collisional activation) were set to 25–30% of 5 V, which corresponds to approximately 0.65 to 0.72 V in the laboratory frame of reference using the current instrument calibration. The activation Q setting (used to adjust the q parameter for the precursor ion during the CID experiment) was 0.30 and activation times of 30 ms were used.

To determine the extent to which ions undergo D for H back exchange while in the ion trap, product ions generated by CID were isolated and stored, without imposed collisional activation, for periods ranging from 10 ms to 1 sec. During the isolation time, ions may react with H_2O present as a contaminant in the vacuum system. Previous experiments have established that an H_2O partial pressure of *ca.* 1.0×10^{-6} exists regardless of the ESI spray solution used, and this H_2O has been used to study intrinsic hydration rates of gas-phase metal complexes.[58]

Fourier-transform mass spectrometry

A custom Fourier transform ion cyclotron resonance (FT-ICR-MS) mass spectrometer at the FOM Institute for Plasma Physics in Nieuwegein, The Netherlands was used for the IRMPD experiments. The mass spectrometer is equipped with a commercial Z-spray electrospray ionization source (Micromass, Manchester, UK) that produces ions at atmospheric pressure in a spray plume orthogonal to a sampling cone. Specific ESI operating parameters such as spray voltage, cone voltage and ion transfer lens voltages and block and nitrogen gas temperatures were adjusted empirically to maximize formation and transfer of ions to the ion cyclotron resonance cell. Peptide solutions were created as described above for the ion trap mass spectrometry studies.

The McLafferty rearrangement of the native or deuterium-exchanged peptides was induced by raising the cone voltage to cause in-source fragmentation. The resulting free-acid forms of the peptides were accumulated in an external hexapole for ~500 ms prior to being injected into the ICR cell *via* a 1 m

octapole ion guide. Rapid switching of the DC bias of the octopole during the ion transfer allows for capture of the ions in the ICR cell without the use of a gas pulse, thus avoiding collisional heating of the ions.[46] Product ions resulting from McLafferty rearrangement induced in the ESI source region were detected in the mass spectrum, and were isolated for IRMPD study using a stored waveform inverse Fourier transform (SWIFT) pulse[59] which ejected all species except those having the desired mass.

Infrared multiple photon dissociation (IRMPD)

Infrared spectra were collected by monitoring the efficiency of IRMPD as a function of laser wavelength. After mass-selective isolation, the precursor ions are irradiated using ten FELIX macropulses (40 mJ per macropulse, 5 μs pulse duration, bandwidth 0.2–0.5% of central λ). IRMPD occurs through non-coherent absorption of tens to hundreds of IR photons when the laser frequency matches a vibrational mode of the gas-phase ion. The energy is distributed over all vibrational modes by intramolecular vibrational redistribution (IVR), which allows the energy of each photon to be "relaxed" prior to the absorption of the next photon, and thus allows promotion of the ion's internal energy to the dissociation threshold.[60] Prior studies have shown that the infrared spectra obtained using IRMPD are comparable to those obtained using linear absorption techniques.[61]

To produce infrared spectra, the free electron laser was scanned in 0.02 to 0.04 μm increments between 5.5 and 8.5 μm, with measurement of product ion and un-dissociated precursor ion intensities using the excite/detect sequence of the FT-ICR-MS[62] after irradiation with FELIX. The IRMPD yield is normalized to the total ion yield, and corrected for variations in FELIX power over the spectral range.

Molecular structure and frequency calculations

All geometry optimizations were performed using the hybrid B3LYP functional.[63,64] Optimization of a wide range of potential conformational isomers of the McLafferty rearrangement products, $(NicGOH+H)^+$ and $(BetGOH)^+$, was initiated using the relatively small 3-21g* basis set. While the various isomers were all found to be stationary points, not all may be expected to form under the conditions used in the present experiments. For example, structures which must form in gas-phase through *cis–trans* isomerizaton of the amide bond are expected to have significant activation barriers. Minimized geometries from calculations at the B3LYP/3-21g* level of theory were then re-optimized using the 6-311+g(d,p) basis set. Frequency calculations were carried out at the B3LYP/6-311+g(d,p) level of theory. Vibrational spectra for the isotope-labeled peptides were calculated using the freq = read isotopes command, which in the Gaussian program incorporates specified isotopes into frequency calculations for optimized structures. For comparison to the experimentally derived spectra, the frequencies generated by DFT were scaled by a factor of 0.98. As discussed below, the B3LYP functional, and the basis sets and scaling factor employed, provided good general agreement with the experimental IRMPD spectra. As the goal here was to use the calculations to assign probable ion structures and assist with interpretation of the IRMPD spectrum, rather than assess the absolute accuracy of theoretical methods, alternative functionals and models were not used, nor was calculation of dissociation and reaction transition state energies carried out. All DFT calculations were performed using the Gaussian 03 group of programs.[65]

Results

Ion trap collision-induced dissociation of $(NicGOtBu+H)^+$ and $(BetGOtBu)^+$ and generation of H isotope label by McLafferty-type rearrangement

Model systems with nicotinic acid or betaine at the N-terminal sequence position were chosen, in part, for this study to test the use of the residues to fix the charge site. As noted earlier, there is both theoretical[11] and experimental, including IRMPD,[12] evidence to support a mix of protonation sites for gas-phase peptide ions. One goal of our research program is to study the influence of sequence on intrinsic peptide conformation, and for such studies it will be important to minimize the tendency for the added charge-bearing species (*i.e.* proton or metal ion) to alter conformation in the gas-phase structure. The initial hypothesis for the NicGO*t*Bu system was that protonation would occur on the pyridine ring, thus preventing the added proton from causing a change in conformation by migrating to and interacting with multiple amide carbonyl O atoms. The betaine residue instead contains a fixed positive charge because of the quaternary nitrogen.

Tandem mass spectra generated from $(NicGOtBu+H)^+$ using the quadrupole ion trap mass spectrometer are shown in Fig. 1. Similar results, in general, were observed for CID of $(BetGOtBu)^+$, and the observations for $(NicGOtBu+H)^+$ are discussed here because they are representative of both systems. Spectra for $(BetGOtBu)^+$ and $(BetGOH)^+$ are provided in Fig. S1 of the ESI.† The only dissociation pathway observed following isolation and CID of $(NicGOtBu+H)^+$ at m/z 237 (MS/MS stage, Fig. 1a) was elimination of 56 mass units (u), which is attributed to loss of isobutene from the *tert*-butyl ester group through McLafferty rearrangement (part a of Scheme 1). The rearrangement furnishes the free-acid form of protonated nicotinyl-glycine, $(NicGOH+H)^+$, at m/z 181. Two pathways were observed following subsequent CID of $(NicGOH+H)^+$ (MS^3 stage, Fig. 1b): a minor pathway that involved formation of an ion at m/z 163 through elimination of 18 u (H_2O), and a major pathway for which the neutral loss was 46 u (H_2O+CO) to furnish an ion at m/z 135.

Using the conventional nomenclature for identification of peptide CID product ions,[66,67] losses of 18 and 46 u correspond to formation of the b_2^+ and a_2^+ species, respectively, as shown in Scheme 1 for $(NicGOtBu+H)^+$. Within the context of the "oxazolone" pathway proposed to explain the general dissociation of protonated peptides,[2,3,26] b_2^+ is an oxazolinone generated by nucleophilic attack upon the C-terminal carbonyl C atom, with associated intramolecular transfer of an amide-position H atom. The oxazolinone then opens, with elimination of CO, to produce a_2^+. Mechanistic studies strongly suggest that the b_n^+ species are cyclic products rather than linear acyllium-type ions.[2,3] CID (MS^3 stage, spectrum

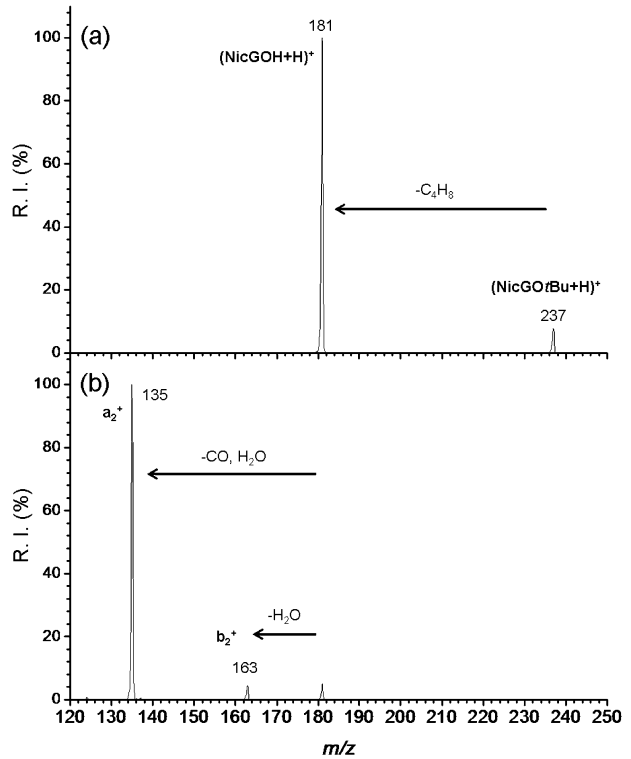

Fig. 1 Tandem mass spectra starting from the protonated nicotinyl-glycine-*tert*-butyl ester $(NicGOtBu+H)^+$ using the quadrupole ion trap mass spectrometer: (a) dissociation of $(NicGO\textit{t}Bu+H)^+$; (b) dissociation (MS^3 stage) of $(NicGOH+H)^+$, product resulting from McLafferty rearrangement.

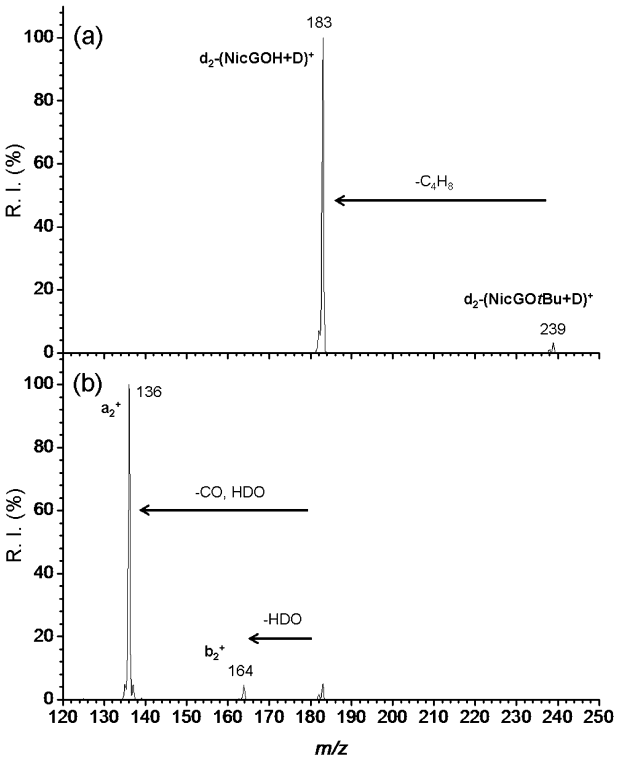

Fig. 2 Tandem mass spectra starting from fully deuterium-exchanged nicotinyl-glycine-*tert*-butyl ester d_2-$(NicGOtBu+H)^+$ using the quadrupole ion trap mass spectrometer: (a) dissociation of d_2-$(NicGO\textit{t}Bu+H)^+$; (b) dissociation (MS^3 stage) of d_2-$(NicGOH+H)^+$, product resulting from McLafferty rearrangement.

not shown) of the m/z 163 product ion generated exclusively the a_2^+ species at m/z 135, consistent with the stepwise formation of a_2^+ from NicGOH.

An alternative pathway for elimination of H_2O is a retro-Ritter or retro-Koch type reaction, as initially proposed by O'Hair and coworkers,[68] which involves elimination of an amide position O atom. Such a pathway is particularly prominent in the dissociation of metal (Li^+ and Na^+) cationized peptide esters,[29,69] and thus was also considered in the present study. To determine the most probable mechanism by which the elimination of H_2O occurs, CID of protonated $(NicGOMe+H)^+$ (m/z 195) was examined (results not shown). CID of this species generated b_2^+ at m/z 163, and a_2^+ at m/z 135 (product ion m/z ratios identical to those observed for NicGOH) *via* elimination of 32 and 60 u, respectively: these neutral losses are consistent with a pathway analogous to that shown in Scheme 1, in that it begins with elimination of CH_3OH from the C-terminus of $(NicGOMe+H)^+$, and is followed by elimination of CO. Comparison of CID results for NicGOH and NicGOMe suggests that the elimination of H_2O from the former occurs at the C-terminus, and thus represents generation of b_2^+.

The mass spectra shown in Fig. 2 were generated from NicGO*t*Bu after incubation in a mixture of D_2O and CH_3OD to induce solution-phase H/D exchange. As shown in Fig. 2a, CID2,100 (MS/MS stage) of d_2-$(NicGOtBu+H)^+$ (2 D atoms, at the ring N and amide N positions) at m/z 239 caused loss of 56 u, through McLafferty rearrangement and transfer of H, to furnish d_2-$(NicGOH+H)^+$ at m/z 183. Subsequent CID (Fig. 2b) of d_2-$(NicGOH+H)^+$ caused elimination of 19 u (HDO) to create b_2^+, and formation of a_2^+ at m/z 136 through loss of 47 u (HDO and CO). Similar dissociation behavior was observed for d_1-$(BetGO\textit{t}Bu)^+$ and d_1-$(BetGO\textit{t}H)^+$, for which CID spectra are provided in Fig. S2 of the ESI.†

The loss of HDO and CO following CID of the deuterium-exchanged forms of nicotinyl-glycine and betaine-glycine clearly demonstrates that an H atom is transferred from the departing butene neutral to the free-acid product ion following McLafferty-rearrangement, consistent with the earlier study of metal-cationized versions of acetylated peptide *tert*-butyl esters.[32] The free-acid forms of the peptides (the products resulting from McLafferty rearrangement) were isolated and stored in the ion trap mass spectrometer, without imposed collision activation, for periods ranging from 10 msec to 1 sec (spectra not shown). This experiment was performed to probe the tendency for D for H back exchange through collisions with ubiquitous H_2O in the ion trap. The test for back-exchange was conducted to ensure that the species generated after McLafferty rearrangement would not be susceptible to significant HDX that might occur through ion-molecule reactions with H_2O present in the ion transfer lenses in the FTICR instrument interfaced to the free-electron laser. In the quadrupole ion trap, for the isolation times used, and exposure to *ca.* 1×10^{-6} torr of H_2O,[55] no D for H back-exchange was observed. This observation suggests that the tendency for

exchange in the FTICR instrument is negligible, which is consistent with the IRMPD results discussed below.

Infrared multiple-photon photodissociation of $(NicGOH+H)^+$ and $(BetGOH)^+$

Several potential conformations of protonated NicGOH, produced by DFT (B3LYP/6-311+g(d,p)), are shown in Fig. 3 and 4. The relative energies of each species are provided in Table 1. The lowest energy conformation predicted for $(NicGOH+H)^+$ by DFT, **Nic_a**, is one in which the peptide is protonated at the ring N atom of the nicotinic acid residue, and includes a hydrogen bonding interaction between the H atom of the amide group and the C-terminal carbonyl O atom.

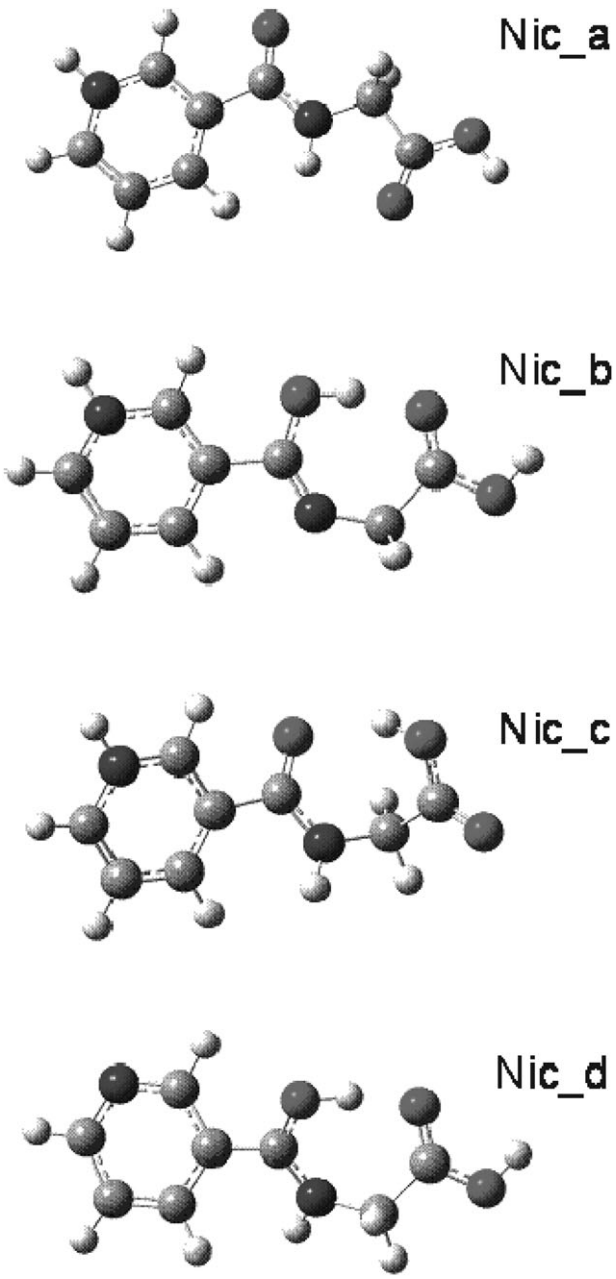

Fig. 3 Potential conformations (**Nic_a**, **Nic_b**, **Nic_c** and **Nic_d**) for $(NicGOH+H)^+$ as determined using DFT (B3LYP/6-311+g(d,p)).

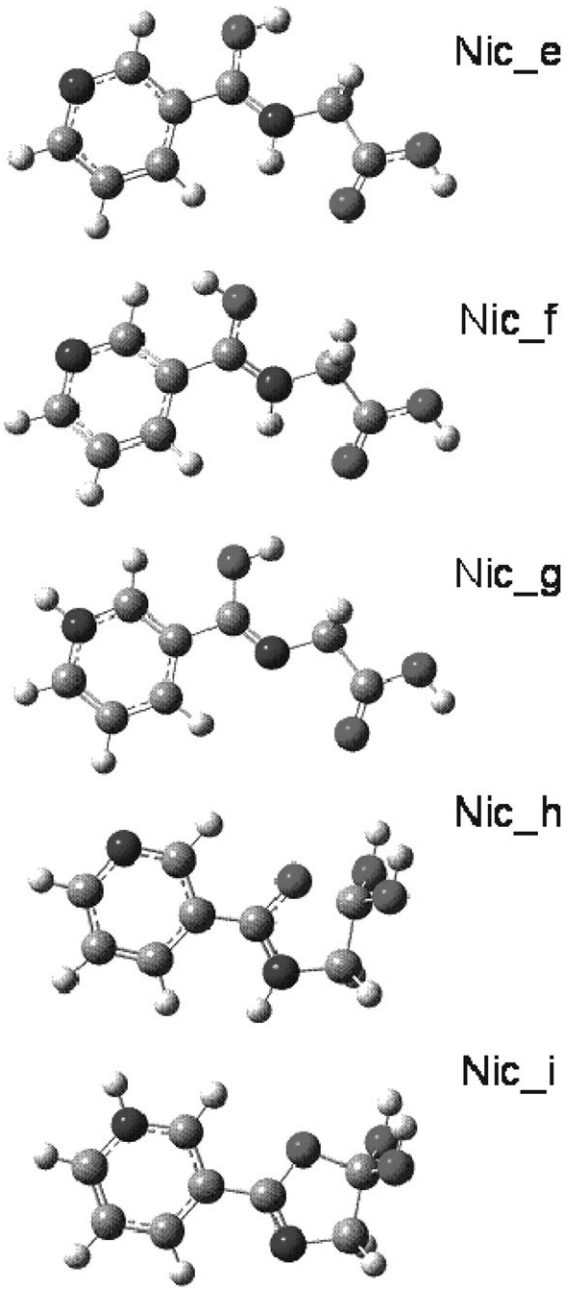

Fig. 4 Potential conformations (**Nic_d**, **Nic_e**, **Nic_f**, **Nic_g** and **Nic_h**) for $(NicGOH+H)^+$ as determined using DFT (B3LYP/6-311+g(d,p)).

Several structures that feature a proton "solvated" by interactions with the two carbonyl groups, **Nic_b**, **Nic_c** and **Nic_d**, were identified, and their relative energies are ~8–12 kcal mol^{-1} higher in energy than **Nic_a**. Other potential conformations that feature single amide O protonation, **Nic_e**, **Nic_f** and **Nic_g**, were all found to be at least 12 kcal mol^{-1} higher in energy. Two structures in which nucleophilic attack and cyclization has occurred were also identified (**Nic_h** and **Nic_i**); these species were >20 kcal mol^{-1} higher than **Nic_a**.

Upon on-resonance irradiation using the FEL, both $(NicGOH+H)^+$ and $(BetGOH)^+$ eliminate H_2O and H_2O+CO, and these photofragment ions were used to

Table 1 Relative energies of $(NicGOH+H)^+$ conformational isomers

Structure	Electronic energy/E_h	Zero point correction/E_h	ZPE corrected energy/E_h	ΔE/kcal mol^{-1}
Nic_a	−645.42760375	0.172342	−645.255262	0
Nic_b	−645.41396927	0.171945	−645.242025	+8.31
Nic_c	−645.41026594	0.172963	−645.237303	+11.27
Nic_d	−645.40820377	0.171706	−645.236497	+11.78
Nic_e	−645.40126874	0.171160	−645.230108	+15.78
Nic_f	−645.40673397	0.171548	−645.235186	+12.60
Nic_g	−645.40215344	0.171161	−645.230992	+15.23
Nic_h	−645.38800499	0.170890	−645.217115	+23.94
Nic_i	−645.38696168	0.171611	−645.215350	+25.05

generate the IRMPD spectra. Fig. 5 compares the experimental IRMPD result for native (no deuterium exchange) $(NicGOH+H)^+$ to theoretical spectra for the four lowest energy conformations, **Nic_a** through **Nic_d**. Comparisons between the experimental spectrum and the theoretical spectra for structures **Nic_e** through **Nic_h** are provided in Fig. S3 of the supporting information. As noted earlier, the computed spectra are scaled by a factor 0.98 for direct comparison to the IRMPD spectrum.

As is apparent in Fig. 5 and S3, the best match to the IRMPD spectrum, both in terms of the positions of the respective absorption frequencies and their relative intensities, is the lowest energy structure **Nic_a**. Comparison to the DFT calculations allows assignment of the absorptions at *ca.* 1770 and 1710 cm^{-1} to the C=O stretches of the acid and amide groups, respectively. The absorption at *ca.* 1500 cm^{-1} corresponds to the amide II band, while the weaker absorption at *ca.* 1400 cm^{-1} is assigned to the C–C backbone stretch focused at the C-terminal G residue. Significant populations of the $(NicGOH+H)^+$ conformational isomers which feature solvation of a proton by amide carbonyl groups (**Nic_b**, **Nic_c** and **Nic_d**), can be ruled out based on the poorer agreement between the IRMPD and theoretical spectra in both the amide I and amide II regions.

Potential conformations of gas-phase $(BetGOH)^+$ are shown in Fig. 6, and the relative energies of the species are

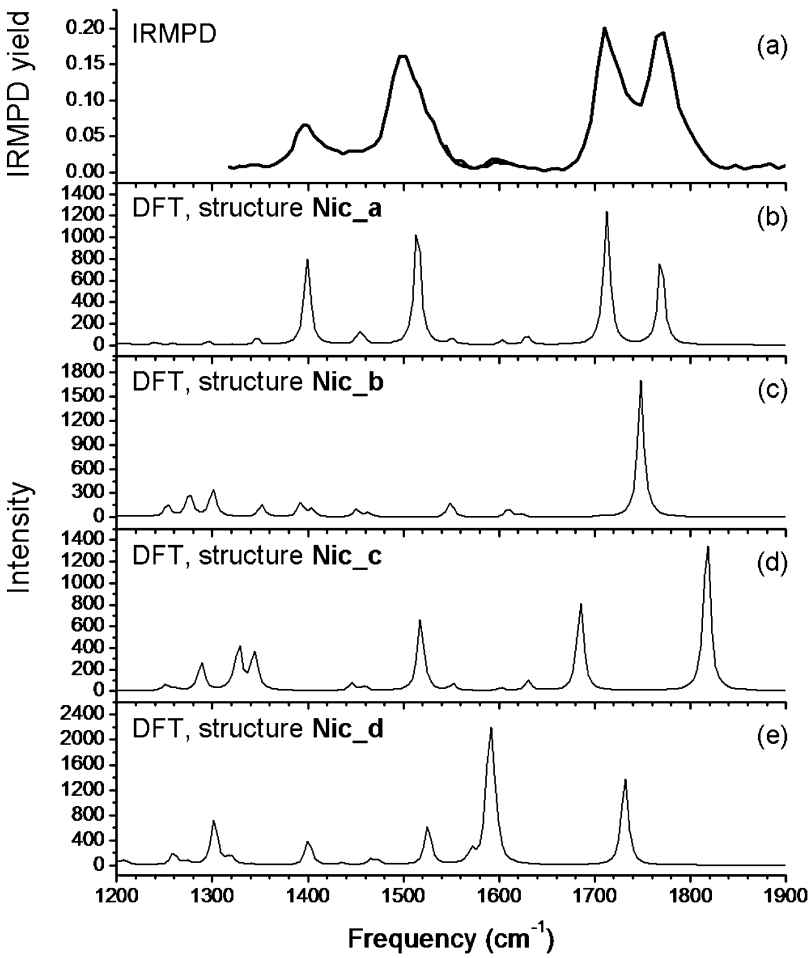

Fig. 5 Comparison between IRMPD spectrum generated from $(NicGOH+H)^+$ (a) and theoretical spectra based on DFT calculations for structures: (b) Nic_a, (c) Nic_b, (d) Nic_c and (e) Nic_d. Conformations of Nic_a, Nic_b, Nic_c and Nic_d are provided in Fig. 3.

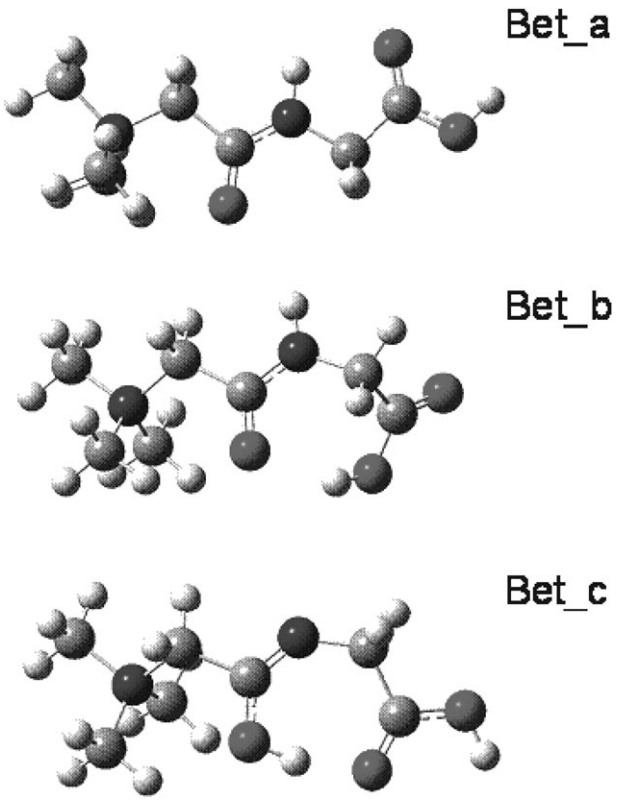

Fig. 6 Potential conformations for $(BetGOH)^+$ as determined using DFT (B3LYP/6-311 + g(d,p)).

provided in Table 2. The lowest energy conformation, **Bet_a**, is extended and features a hydrogen bonding interaction between the H atom of the amide group and the C-terminal carbonyl O atom. The structure in which the acid OH proton instead participates in a hydrogen bonding interaction with the amide carbonyl O atom, **Bet_b**, is several kcal mol^{-1} higher in energy. Fig. 7 compares the experimental IRMPD spectrum of native (no deuterium exchange) $(BetGOH)^+$ to those predicted for species **Bet_a** and **Bet_b**. As is apparent in Fig. 7, the best agreement between theory and experiment for the non-exchanged $(BetGOH)^+$ is for the species **Bet_a**. As in the case of $(NicGOH + H)^+$, comparison of the IRMPD spectrum generated from $(BetGOH)^+$ to the DFT calculations allows assignment of the absorptions at *ca.* 1770 and 1710 cm^{-1} to the C═O stretches of the acid and amide groups, respectively. The absorption at *ca.* 1500 cm^{-1} corresponds to the amide II band, while the weaker absorption at *ca.* 1400 cm^{-1} is assigned to the C–C backbone stretch focused at the C-terminal G residue. The amide II region is more congested for $(BetGOH)^+$ because of the addition of absorptions attributable to the tri-methyl amino group.

Fig. 8a shows the the IRMPD spectrum derived from d_2-$(NicGOH + H)^+$ that was generated by McLafferty rearrangement of the deuterium-exchanged form of $(NicGO\textit{t}Bu + H)^+$. As demonstrated by the ion-trap CID results, McLafferty rearrangement causes transfer of an H atom to the peptide, presumably to the C-terminal acid group (the amide and pyridine ring N atoms carry D atoms as a result of solution-phase H/D exchange). The theoretical spectra shown in Fig. 8b–d are those predicted for d_2-$(NicGOH + H)^+$ with different arrangements of the two D and one H atom in exchangeable positions: 8b shows the calculations for ring D, amide D and acid H; 8c shows the results for ring D, amide H and acid D and 8d shows the results for ring H, amide D and acid D. Adoption of isotope configurations modeled for 8c and 8d represent cases in which the H label generated by McLafferty rearrangement "scrambles" with the D atoms at the other exchangeable sites.

Comparison of spectra in Fig. 8 suggests that the best match between theory and experiment is for the structure that features the H atom at the C-terminal acid group and with D at the ring N and amide N positions. As indicated in Fig. 8b, DFT predicts that placement of a D atom at the amide N position of $(NicGOH + H)^+$ shifts the characteristic amide II band by *ca.* 70 cm^{-1} to ~1430 cm^{-1}, which places the absorption in the high-frequency shoulder of the IRMPD peak in the region of 1360–1460 cm^{-1}. The major component in this same region is attributed to C–C stretches of the peptide backbone. It is also apparent from Fig. 8 that placement of D at the amide position has little influence on the position or intensity of the absorptions in the amide I region.

The presence of a significant population of gas-phase ions for which the H atom label has migrated to the amide N position would presumably be identified by an intense absorption in the vicinity of 1520 cm^{-1}, as predicted in the spectrum shown for the labeled peptide in Fig. 8c and as observed in Fig. 5a and b for the non-labeled version of $(NicGOH + H)^+$. Migration of the H atom to the pyridyl ring, and a D atom to the C-terminal acid group, would presumably generate 2 absorptions of nearly equal intensity in the region of 1360–1460 cm^{-1}, and separated by *ca.* 60 cm^{-1}. While the two predicted absorptions fall within the range of the peak between 1360 cm^{-1} and 1460 cm^{-1} in the IRMPD spectrum, one would expect that contribution from the isotopic isomer modeled in Fig. 8d would lead to a broader feature in this region, as well as a third strong absorption near 1240 cm^{-1}.

Fig. 9 shows the comparison between the IRMPD spectrum derived from the d_1-$(BetGOH)^+$ ion generated by McLafferty rearrangement from the deuterium-exchanged form of the peptide. For the cationic $(BetGOH)^+$ peptide there are only two exchangeable sites, the amide N and acid OH groups. The spectra shown in Fig. 9b and c are those predicted for d_1-$(BetGOH)^+$ with different arrangements of the D and H

Table 2 Relative energies of $(BetGOH)^+$ conformational isomers

Structure	Electronic energy/E_h	Zero point correction/E_h	ZPE corrected energy/E_h	ΔE/kcal mol^{-1}
Bet_a	−610.92899952	0.233636	−610.695364	0
Bet_b	−610.91166897	0.234249	−610.677420	+11.260
Bet_c	−610.90728477	0.246720	−610.673821	+13.520

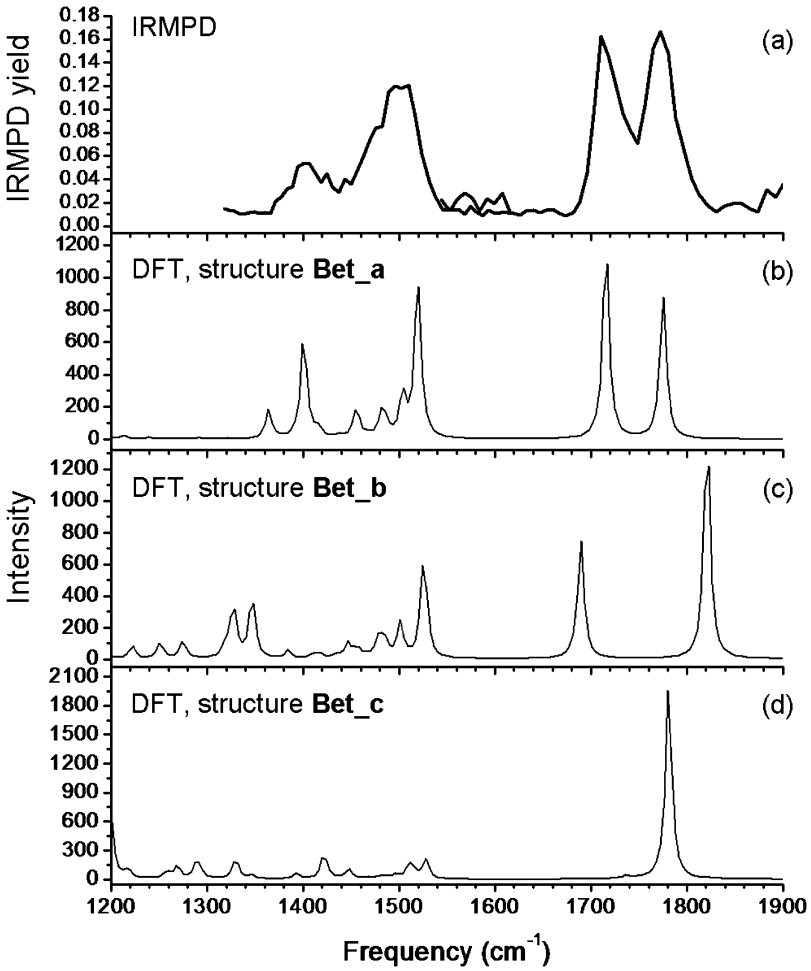

Fig. 7 Comparison between IRMPD spectrum generated from BetGOH (a) and theoretical spectra based on DFT calculations for structures: (b) Bet_a and (c) Bet_b. Conformations of Bet_a and Bet_b are provided in Fig. 6.

atoms: 9b shows the calculations for amide D and acid H; 9c shows the results for amide H and acid D. As for the d_2-(NicGOH + H)$^+$ cation, the best agreement between the theoretical spectra and the IRMPD spectrum for the deuterium exchanged form of (BetGOH)$^+$ is for the species with the H atom located on the free acid moiety.

Discussion

Previous mass spectrometric studies have conclusively established that an H atom from a γ-position C atom is transferred during McLafferty rearrangement.[70,71] In the IRMPD study reported here, the vibrational spectra generated from CID products of isotope labeled peptide esters clearly show that the H atom transferred during the rearrangement is retained at the C-terminal acid group, entirely consistent with the mechanism as originally proposed. To the best of our knowledge, this represents the first study of the reaction using vibrational spectroscopy to probe the structures of the product ions.

Comparison of WS-IRMPD data to theoretical spectra for different isotopic isomers of either d_2-(NicGOH + H)$^+$ or d_1-(BetGOH)$^+$ strongly suggest that minimal migration or scrambling of the H isotope label, generated by McLafferty rearrangement, occurs on the time scales (< sec) accessed in the experiments reported here. For either system, scrambling of the isotope label could conceivably occur through isomerization, tautomerization and adoption of structures in which intramolecular hydrogen bonding interactions arise between amide carbonyl groups. DFT calculations performed using small, model peptides suggest that tautomerization to produce such structures should be energetically feasible, and may form used in ion-trapping instruments during peptide CID.[72] The migration of protons across a peptide backbone occurs through multiple cyclization and proton transfer steps between amide carbonyl groups: these cyclic intermediates and transition states for proton transfer have all been found to lie below the threshold for dissociation for small peptides by DFT calculations.[11,72] Thus the lack of migration and transfer of the H atom in the present study suggests that the internal energy of the product ions, after McLafferty rearrangement was not sufficiently high to overcome the barriers either to tautomerization or proton transfer.

Beyond confirming the rearrangement reaction mechanism, the results of this study have important implications for the use of *in situ* generation of an isotope label/tracer for the study of intramolecular proton migration. In an earlier study of

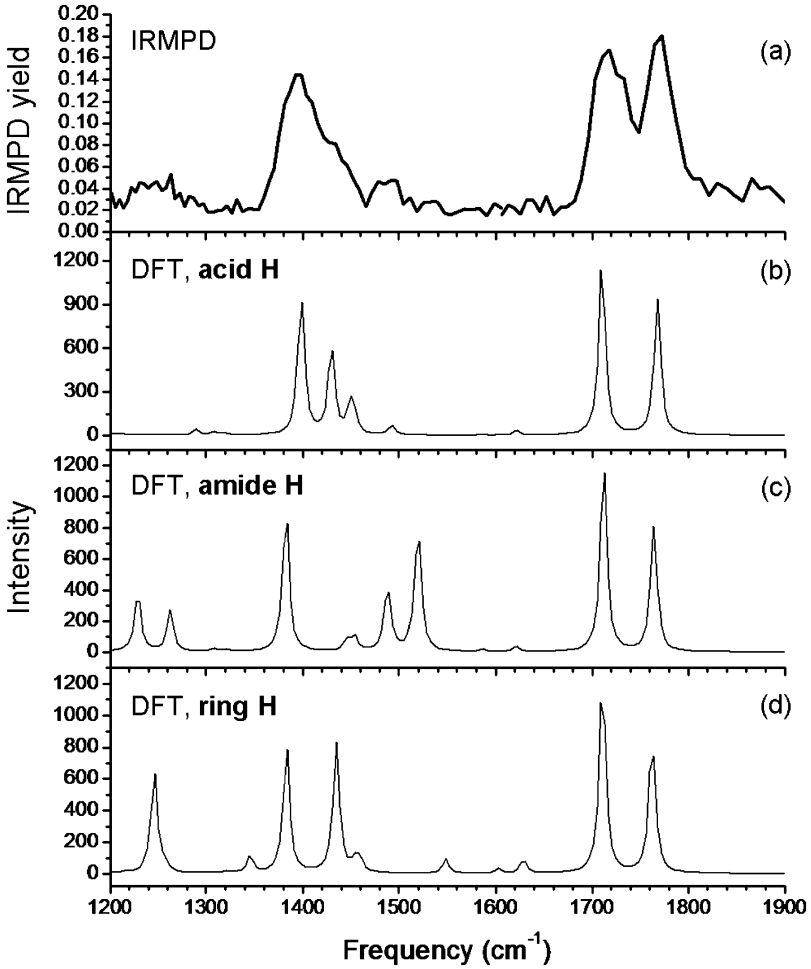

Fig. 8 Comparison between IRMPD spectrum generated from d_2-$(NicGOH+H)^+$ (a), and theoretical spectra based on DFT calculations for 3 different labeled isomers: (b) ring D, amide D and acid H; (c) ring D, amide H and acid D and (d) ring H, amide D and acid D. The conformation used to model the isomers was **Nic_a**, Fig. 3.

migration/scrambling using the isotope label method and metal-cationzed peptides, intramolecular scrambling of H and D during CID of peptide ions was exposed by the splitting of specific sequence ions into isotopic peaks.[28] By incorporating sarcosine at various sites within a model AcGGG-OH motif it was clear that the amount of peak splitting, and thus isotope scrambling, was dependent on the number and position of possible exchange sites. One important assumption made in the prior study was that the isotope tracer, once generated by McLafferty rearrangement, remained at the C-terminal acid group. Subsequent scrambling was then assumed to occur during the dissociation reactions to produce specific sequence ions. The present results suggest that the initial assumption was correct, and that the splitting of specific sequence ions into isotopic peaks was due to the scrambling of protons during the dissociation reaction. In future campaigns, work will focus on combining generation of isotope label by McLafferty rearrangement and spectroscopic investigation using the IRMPD method to study intramolecular proton migration in the same metal cationized peptide systems employed in the earlier study, as well as in larger protonated peptides, to map the extent to which H atom migration occurs during CID reactions.

As noted earlier, the $(NicGOtBu+H)^+$ and $(BetGOtBu)^+$ cations were chosen for this study to test the use of functional groups to fix the charge site within model peptide systems. To study the intrinsic influence of sequence on peptide conformation, it will important to minimize any effect of the added proton, or metal ion, on structure. The initial hypothesis for the NicGO*t*Bu system was that protonation would occur on the pyridine ring, thus keeping the proton from effecting a change in conformation by interacting with the amide carbonyl O atoms. This hypothesis is supported by the IRMPD study of $(NicGOH+H)^+$, for which the best comparison to theoretical spectra is for the ring-protonated species. Preliminary investigations using IRMPD suggest that nicotinic acid can be used to sequester the added proton at the N-terminus of larger peptides.[73] In the case of the $(BetGOtBu)^+$ cation, the present results demonstrate that IRMPD can be used with a peptide in which the charge site is permanently fixed to the N-terminus, thus allowing for potential spectroscopic investigation of charge-remote fragmentation reactions.

Conclusions

Using wavelength-selective IRMPD we have investigated transfer of an H atom by McLafferty rearrangement for two

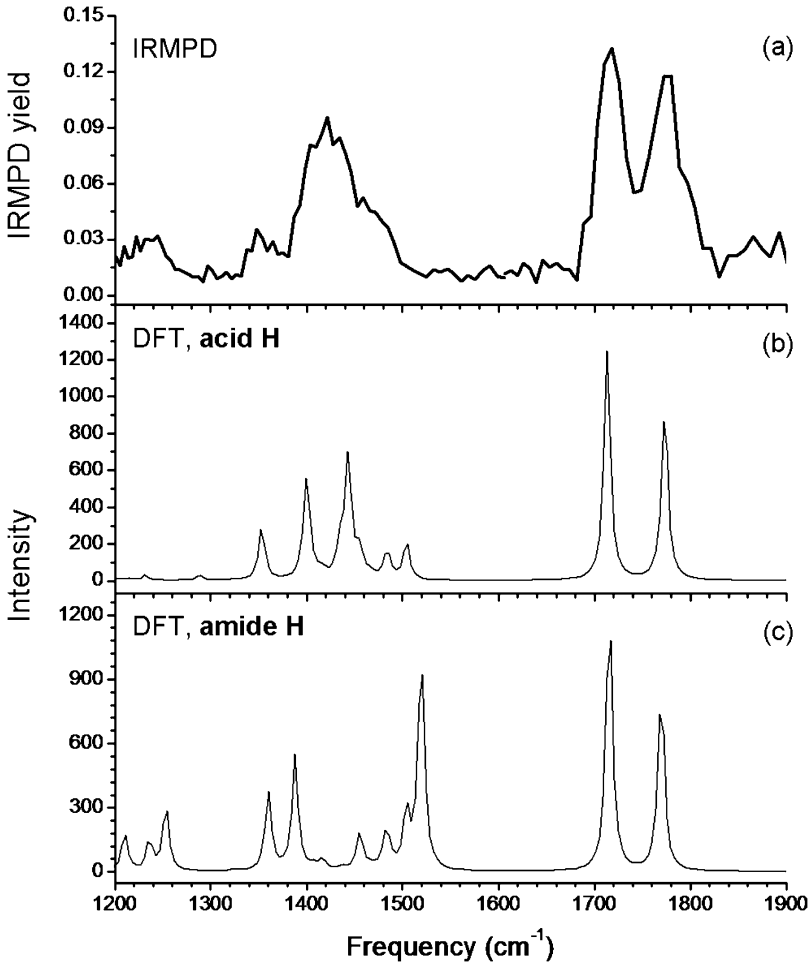

Fig. 9 Comparison between IRMPD spectrum generated from d_1-$(BetGOH)^+$ (a) and theoretical spectra based on DFT calculations for 3 different labeled isomers: (b) amide D and acid H and (c) amide H and acid D. The conformation used to model the isomers was **Bet_a**, Fig. 5.

model peptide systems, protonated nicotinyl-glycine-*tert*-butyl ester and the cationic betaine-glycine-*tert*-butyl ester. McLafferty rearrangement was used to generate the free-acid forms of the respective model peptides through transfer of an H atom and elimination of butene. The resulting peptide ions were then subjected to wavelength-selective IRMPD to produce vibrational spectra from 1200–1900 cm^{-1}. Comparison with DFT-generated spectra allowed definitive assignment of absorption bands corresponding to the free-acid carbonyl, amide I and amide II stretches, and enabled assignment of ion structure. For the nicotinyl-glycine system, the best match between IRMPD and theoretical spectra, both in terms of the respective absorption frequencies and relative intensities, is for a conformational isomer that is protonated at the pyridine ring N atom, and includes an intramolecular hydrogen bonding interaction between the amide position H atom and the C-terminal carbonyl O atom. For the betaine-glycine system, the best agreement between theory and experiment was for a linear conformer with a stabilizing intramolecular hydrogen bond similar to that for the analogous nicotinyl-glycine system.

The intramolecular transfer of the H atom by McLafferty rearrangement, and in particular, the potential scrambling of the exchangeable H atoms, was proved using the model peptide *tert*-butyl esters incubated in a mixture of D_2O and CH_3OD to induce H/D exchange. For the deuterium exchanged peptide ester, CID and McLafferty rearrangement produces a heterogeneous isotopically labeled peptide ion containing two D atoms and one H atom at exchangeable sites. Comparison of the IRMPD results to theoretical spectra for different isotope labeled isomers clearly shows that the H atom is situated at the C-terminal acid group and migration to amide positions is minimal on the time scale of the experiment. Thus scrambling of H atoms situated on exchangeable sites is not occurring to any significant degree.

While the general features of the McLafferty rearrangement have been inferred from several mechanistic studies using isotope labeling and mass spectrometry (and thus made the system a good prototype for the IRMPD investigation), to the best of our knowledge this is the first infrared spectroscopic investigation of the structures of the closed-shell product ions, which are in accord with the hypothesized reaction pathway. In addition to demonstrating that the IRMPD approach can be used to study H atom transfer within discrete ions, the results suggest that use of the McLafferty rearrangement for peptide esters could be an effective approach for generation of H-atom isotope tracers, *in situ*, for the investigation of intramolecular proton migration during peptide fragmentation studies.

Acknowledgements

This work was supported in part by a grant from the National Science Foundation (CAREER-0239800) and a First Award from the Kansas Technology Enterprise Corporation/Kansas NSF EPSCoR program. Purchase of the quadrupole ion-trap mass spectrometer was made possible by a grant from the Kansas NSF-EPSCoR program and matching funds from Wichita State University. DFT calculations were performed at Wichita State University using resources of the High-performance Computing Center (HIPECC), a facility supported by the NSF under Grants EIA-0216178 and EPS-0236913 and matching support from the State of Kansas and HIPECC. Work by G. Groenewold is supported by the US Department of Energy, INL Laboratory Directed Research & Development Program under DOE Idaho Operations Office Contract DE AC07 05ID14517. J. Oomens and J. Steill are supported by the Nederlandse Organisatie voor Wetenschappelijk Onderzoek (NWO). Construction and shipping of the FT-ICR-MS instrument was made possible through funding from the National High Field FT-ICR Facility (grant CHE-9909502) at the National High Magnetic Field Laboratory, Tallahassee, FL.

References

1 I. A. Papayannopoulos, *Mass Spectrom. Rev.*, 1995, **14**, 49–73.
2 T. Yalcin, C. Khouw, I. G. Csizmadia, M. R. Peterson and A. G. Harrison, *J. Am. Soc. Mass Spectrom.*, 1995, **6**, 1165–1174.
3 T. Yalcin, I. G. Csizmadia, M. B. Peterson and A. G. Harrison, *J. Am. Soc. Mass Spectrom.*, 1996, **7**, 233–242.
4 M. J. Nold, C. Wesdemiotis, T. Yalcin and A. G. Harrison, *Int. J. Mass Spectrom. Ion Processes*, 1997, **164**, 137–153.
5 B. Paizs, G. Lendvay, K. Vékey and S. Suhai, *Rapid Commun. Mass Spectrom.*, 1999, **13**, 525–533.
6 A. G. Harrison, I. G. Csizmadia and T.-H. Tang, *J. Am. Soc. Mass Spectrom.*, 2000, **11**, 427–436.
7 B. Paizs and S. Suhai, *Rapid Commun. Mass Spectrom.*, 2002, **16**, 375–389.
8 B. Paizs and S. Suhai, *J. Am. Soc. Mass Spectrom.*, 2004, **15**, 103–112.
9 N. C. Polfer, J. Oomens, S. Suhai and B. Paizs, *J. Am. Chem. Soc.*, 2005, **127**, 17154–17155.
10 N. C. Polfer, J. Oomens, S. Suhai and B. Paizs, *J. Am. Chem. Soc.*, 2007, **120**, 5887–5897.
11 C. F. Rodriquez, A. Cunje, T. Shoeib, I. K. Chu, A. C. Hopkinson and K. W. M. Siu, *J. Am. Chem. Soc.*, 2001, **123**, 3006–3012.
12 R. Wu and T. B. Mc Mahon, *J. Am. Chem. Soc.*, 2007, **129**, 11312–11313.
13 J. L. Jones, A. R. Dongré, Á. Somogyi and V. H. Wysocki, *J. Am. Chem. Soc.*, 1994, **116**, 8368–8369.
14 G. Tsaprailis, H. Nair, Á. Somogyi, V. H. Wysocki, W. Zhong, J. H. Futrell, S. G. Summerfield and S. J. Gaskell, *J. Am. Chem. Soc.*, 1999, **121**, 5142–5154.
15 V. H. Wysocki, G. Tsaprailis, L. L. Smith and L. A. Breci, *J. Mass Spectrom.*, 2000, **35**, 1399–1406.
16 C. W. Tsang and A. G. Harrison, *J. Am. Chem. Soc.*, 1976, **98**, 1301–1308.
17 A. G. Harrison and T. Yalcin, *Int. J. Mass Spectrom. Ion Processes*, 1997, **165**, 339–347.
18 O. Burlet, C. Y. Yang and S. J. Gaskell, *J. Am. Soc. Mass Spectrom.*, 1992, **3**, 337–344.
19 K. A. Cox, S. J. Gaskell, M. Morris and A. Whiting, *J. Am. Soc. Mass Spectrom.*, 1996, **7**, 522–531.
20 S. G. Summerfield, A. Whiting and S. J. Gaskell, *Int. J. Mass Spectrom. Ion Processes*, 1997, **162**, 149–161.
21 S. G. Summerfield, K. A. Cox and S. J. Gaskell, *J. Am. Soc. Mass Spectrom.*, 1997, **8**, 25–31.
22 X. Tang and R. K. Boyd, *Rapid Commun. Mass Spectrom.*, 1992, **6**, 651–657.
23 X. Tang, P. Thibault and R. K. Boyd, *Anal. Chem.*, 1993, **65**, 2824–2834.
24 I. P. Csonka, B. Paizs, G. Lendavy and S. Suhai, *Rapid Commun. Mass Spectrom.*, 2000, **14**, 417–427.
25 B. Paizs, I. P. Csonka, G. Lendvay and S. Suhai, *Rapid Commun. Mass Spectrom.*, 2001, **15**, 637–647.
26 B. Paizs and S. Suhai, *Mass Spectrom. Rev.*, 2004, **24**, 508–548.
27 E. R. Talaty, T. J. Cooper, S. Osburn and M. J. Van Stipdonk, *Rapid Commun. Mass Spectrom.*, 2006, **20**, 3443–3455.
28 H. Steen and M. Mann, *Nat. Rev. Mol. Cell Biol.*, 2004, **5**, 699–711.
29 V. Anbalagan, J. N. Patel, G. Niyakorn and M. J. Van Stipdonk, *Rapid Commun. Mass Spectrom.*, 2003, **17**, 291–300.
30 S. De Feyter, E. W.-G. Diau and A. H. Zewail, *Angew. Chem., Int. Ed.*, 2000, **39**, 260–263.
31 T. H. Osterheld and J. I. Brauman, *J. Am. Chem. Soc.*, 1990, **112**, 2104–2106.
32 K. Bulleigh, A. Howard, T. Do, Q. Wu, V. Anbalagan and M. Van Stipdonk, *Rapid Commun. Mass Spectrom.*, 2006, **20**, 227–232.
33 J. Buijs, C. Hagman, K. Hakansson, J. Hinnerk Richter, P. Hakansson and S. Oscarsson, *J. Am. Soc. Mass Spectrom.*, 2001, **12**, 410–420.
34 J. A. A. Demmers, D. T. S. Rijkers, J. Haverkamp, J. A. Killian and A. J. R. Heck, *J. Am. Chem. Soc.*, 2002, **124**, 11191–11198.
35 T. J. D. Jorgensen, H. Gardsvoll, M. Ploug and P. Roepstorff, *J. Am. Chem. Soc.*, 2005, **127**, 2785–2793.
36 T. J. D. Jorgensen, N. Bache, P. Roepstorff, H. Gardsvoll and M. Ploug, *Mol. Cell. Proteomics*, 2005, **4**, 1910–1919.
37 A. H. Harrison and T. Yalcin, *Int. J. Mass Spectrom.*, 1997, **165**, 339–347.
38 R. S. Johnson, D. Krylov and K. A. Walsh, *J. Mass Spectrom.*, 1995, **30**, 386–387.
39 P. L. Ferguson, J. Pan, D. J. Wilson, B. Dempsey, G. Lajoie, B. Shilton and L. Konermann, *Anal. Chem.*, 2007, **79**, 153–160.
40 F. W. McLafferty, Z. Guan, U. Haupts, T. D. Wood and N. L. Kelleher, *J. Am. Chem. Soc.*, 1998, **120**, 4732–4740.
41 K. D. Rand and T. J. D. Jorgensen, *Anal. Chem.*, 2007, **79**, 8686–8693.
42 B. Lucas, G. Gergoire, J. Lemaire, P. Maitre, J. M. Ortega, A. Rupenyan, B. Erimann and J.-P. Schermann, *Phys. Chem. Chem. Phys.*, 2004, **4**, 2659.
43 B. Lucas, G. Gergoire, J. Lemaire, P. Maitre, F. Glotin, J.-P. Schermann and C. Desfrancois, *Int. J. Mass Spectrom.*, 2005, **243**, 97.
44 C. Kapota, J. Lemaire, P. Maitre and G. Ohanessian, *J. Am. Chem. Soc.*, 2004, **126**, 1836.
45 N. C. Polfer, B. Paizs, L. C. Snoek, I. Compagnon, S. Suhai, G. Meijer, G. von Helden and J. Oomens, *J. Am. Chem. Soc.*, 2005, **127**, 8571.
46 N. C. Polfer, J. Oomens, D. T. Moore, G. von Helden, G. Meijer and R. C. Dunbar, *J. Am. Chem. Soc.*, 2006, **128**, 905.
47 N. C. Polfer, R. C. Dunbar and J. Oomens, *J. Am. Soc. Mass Spectrom.*, 2007, **18**, 512.
48 J. M. Bakker, C. Plutzer, I. Hunig, T. Haber, I. Compagnon, G. von Helden, G. Meijer and K. Kleinermanns, *ChemPhysChem*, 2005, **6**, 120–128.
49 I. Compangon, J. Oomens, J. Bakker, G. Meijer and G. von Helden, *Phys. Chem. Chem. Phys.*, 2005, **7**, 13–15.
50 K. Fukui, T. Takada, T. Sumiyoshi, T. Imai and K. Takahashi, *J. Phys. Chem. B*, 2006, **110**, 16111–16116.
51 G. Gergoire, M. P. Gaigeot, D. C. Marinica, J. Lemaire, J. P. Schermann and C. Desfrancois, *Phys. Chem. Chem. Phys.*, 2007, **9**, 3082–3097.
52 A. Simon, L. MacAleese, P. Maitre, J. Lemaire and T. B. McMahon, *J. Am. Chem. Soc.*, 2007, **129**, 2829–2840.
53 M. A. Duncan, *Annu. Rev. Phys. Chem.*, 1997, **48**, 69.
54 M. A. Duncan, *Int. Rev. Phys. Chem.*, 2003, **22**, 407.
55 J. Lemaire, M. Boissel, G. Heninger, G. Mauclaire, G. Bellec, H. Mestdagh, A. Simon, S. Le Caer, J. M. Ortega, F. Glotin and P. Maitre, *Phys. Rev. Lett.*, 2002, **89**, 273002.
56 J. Oomens, B. G. Sarkatov, G. Meijer and G. von Helden, *Int. J. Mass Spectrom.*, 2006, **254**, 1.
57 J. M. Barr and M. J. Van Stipdonk, *Rapid Commun. Mass Spectrom.*, 2002, **16**, 566–578.

58 W. Chien, D. Hanna, V. Anbalagan, G. Gresham, G. Groenewold, M. Zandler and M. J. Van Stipdonk, *J. Am. Soc. Mass Spectrom.*, 2004, **15**, 777–783.
59 A. G. Marshall, T.-C. L. Wang and T. L. Ricca, *J. Am. Chem. Soc.*, 1985, **107**, 7893.
60 V. N. Bagratashvili, V. S. Letokov, A. A. Makarov and E. A. Ryabov, *Multiple Photon Infrared Laser Photophysics and Photochemistry*, Harwood, Chur, Switzerland, 1985.
61 J. Oomens, G. G. M. Tielens, B. G. Sartakov, G. von Helden and G. Meijer, *Astrophys. J.*, 2003, **591**, 968.
62 A. G. Marshall, C. L. Hendrickson and G. S. Jackson, *Mass Spectrom. Rev.*, 1998, **17**, 1.
63 C. T. Lee, W. T. Yang and R. G. Parr, *Phys. Rev. B*, 1988, **37**, 785.
64 A. D. Becke, *J. Chem. Phys.*, 1993, **98**, 5648.
65 M. J. Frisch, G. W. Trucks, H. B. Schlegel, G. E. Scuseria, M. A. Robb, J. R. Cheeseman, J. A. Montgomery, Jr, T. Vreven, K. N. Kudin, J. C. Burant, J. M. Millam, S. S. Iyengar, J. Tomasi, V. Barone, B. Mennucci, M. Cossi, G. Scalmani, N. Rega, G. A. Petersson, H. Nakatsuji, M. Hada, M. Ehara, K. Toyota, R. Fukuda, J. Hasegawa, M. Ishida, T. Nakajima, Y. Honda, O. Kitao, H. Nakai, M. Klene, X. Li, J. E. Knox, H. P. Hratchian, J. B. Cross, V. Bakken, C. Adamo, J. Jaramillo, R. Gomperts, R. E. Stratmann, O. Yazyev, A. J. Austin, R. Cammi, C. Pomelli, J. W. Ochterski, P. Y. Ayala, K. Morokuma, G. A. Voth, P. Salvador, J. J. Dannenberg, V. G. Zakrzewski, S. Dapprich, A. D. Daniels, M. C. Strain, O. Farkas, D. K. Malick, A. D. Rabuck, K. Raghavachari, J. B. Foresman, J. V. Ortiz, Q. Cui, A. G. Baboul, S. Clifford, J. Cioslowski, B. B. Stefanov, G. Liu, A. Liashenko, P. Piskorz, I. Komaromi, R. L. Martin, D. J. Fox, T. Keith, M. A. Al-Laham, C. Y. Peng, A. Nanayakkara, M. Challacombe, P. M. W. Gill, B. Johnson, W. Chen, M. W. Wong, C. Gonzalez and J. A. Pople, *GAUSSIAN 03 (Revision D.01)*, Gaussian Inc., Wallingford, CT, 2004.
66 P. Roepstorff, *Biomed. Mass Spectrom.*, 1984, **11**, 601.
67 K. Biemann, *Meth. Enzymol.*, 1990, **193**, 455–465.
68 G. E. Reid, R. J. Simpson and R. A. O'Hair, *J. Am. Soc. Mass Spectrom.*, 1998, **9**, 945–956.
69 E. R. Talaty, T. J. Cooper, D. L. Piland, D. J. Bateman, A. Syed, W. Stevenson and M. J. Van Stipdonk, *Rapid Commun. Mass Spectrom.*, 2006, **20**, 3007–3017.
70 F. W. McLafferty, *Anal. Chem.*, 1956, **28**, 306.
71 J. Budzikiewicz, C. Fenselau and C. Djerassi, *Tetrahedron*, 1966, **22**, 1391.
72 I. P. Csonka, B. Paizs, G. Lendvay and S. Suhai, *Rapid Commun. Mass Spectrom.*, 2001, **15**, 1457–1472.
73 K. Griffith, C. Chueachavalit, V. Bashyakarla, M. Kullman, G. Groenewold, J. Oomens and M. J. Van Stipdonk, manuscript in preparation.